

Supplementary material

Effect of aqueous-phase processing on aerosol chemistry and size distributions in Fresno, California, during wintertime

Xinlei Ge^A, Qi Zhang^{A,D}, Yele Sun^B, Christopher R. Ruehl^C and Ari Setyan^A

^ADepartment of Environmental Toxicology, University of California, One Shields Avenue, Davis, CA 95616, USA.

^BState Key Laboratory of Atmospheric Boundary Layer Physics and Atmospheric Chemistry, Institute of Atmospheric Physics, Chinese Academy of Sciences, Beijing 100029, P. R. China.

^CEnvironmental Science, Policy, and Management. University of California, 130 Mulford Hall, Berkeley, CA 94720, USA.

^DCorresponding author. Email: dkwzhang@ucdavis.edu

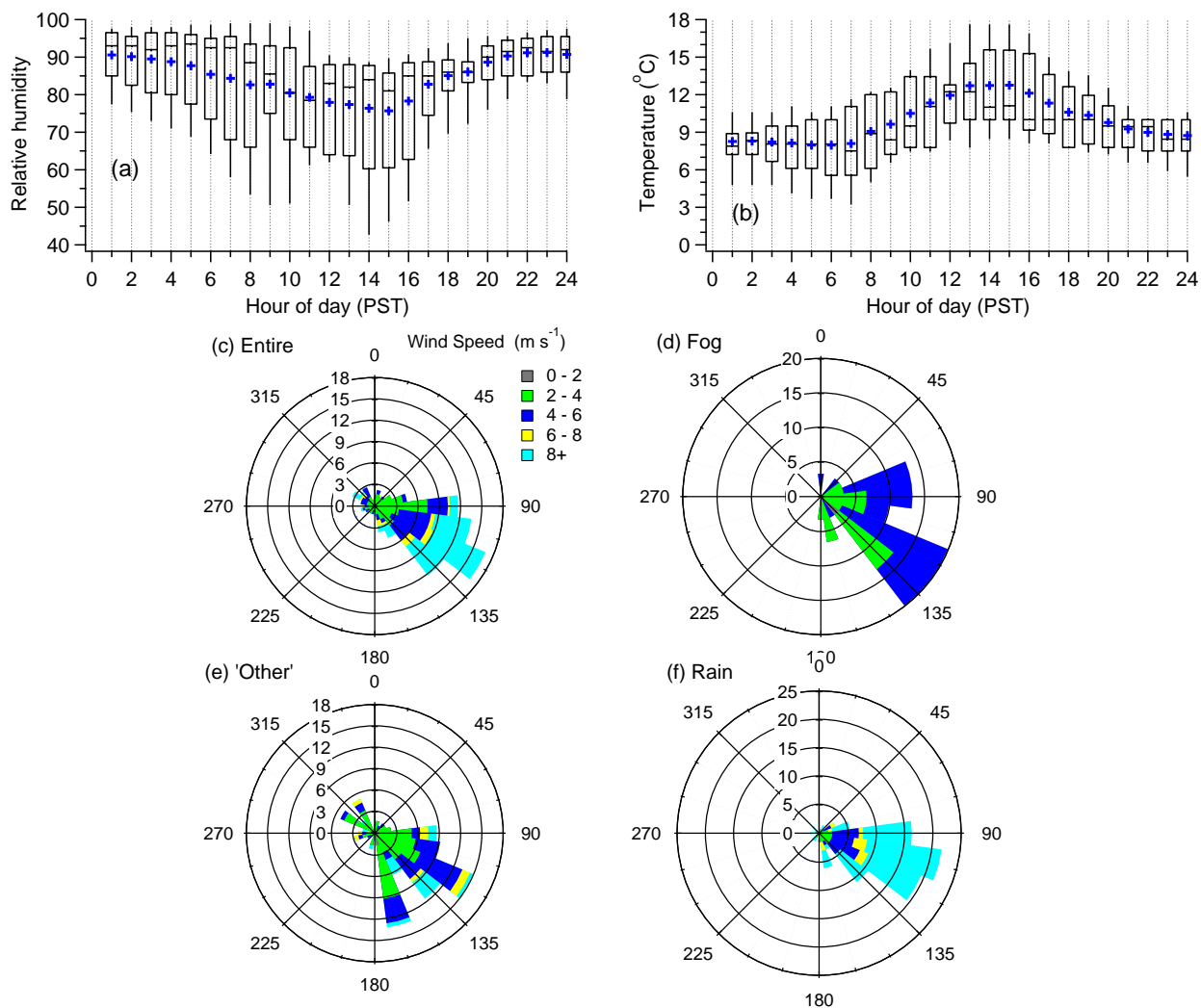


Fig. S1. Box plots of (a) relative humidity and (b) temperature; the whiskers above and below boxes are the 90th and 10th percentiles; the upper and lower boundaries of boxes indicates the 75th and 25th percentiles; the lines in the boxes are median values and the markers indicate the mean values. Wind rose plots of (c) entire campaign, (d) fog periods, (e) 'other' periods and (f) rain periods. The fog periods are identified based on the high liquid water content ($>20 \text{ mg m}^{-3}$); rain periods are differentiated from the precipitation starting in the late afternoon of 17 January until the end of 22 January, plus a short rain event in the early morning of 13 January; periods not classified as these two types are referred to as 'other', as marked in Fig. 3 of the main text.

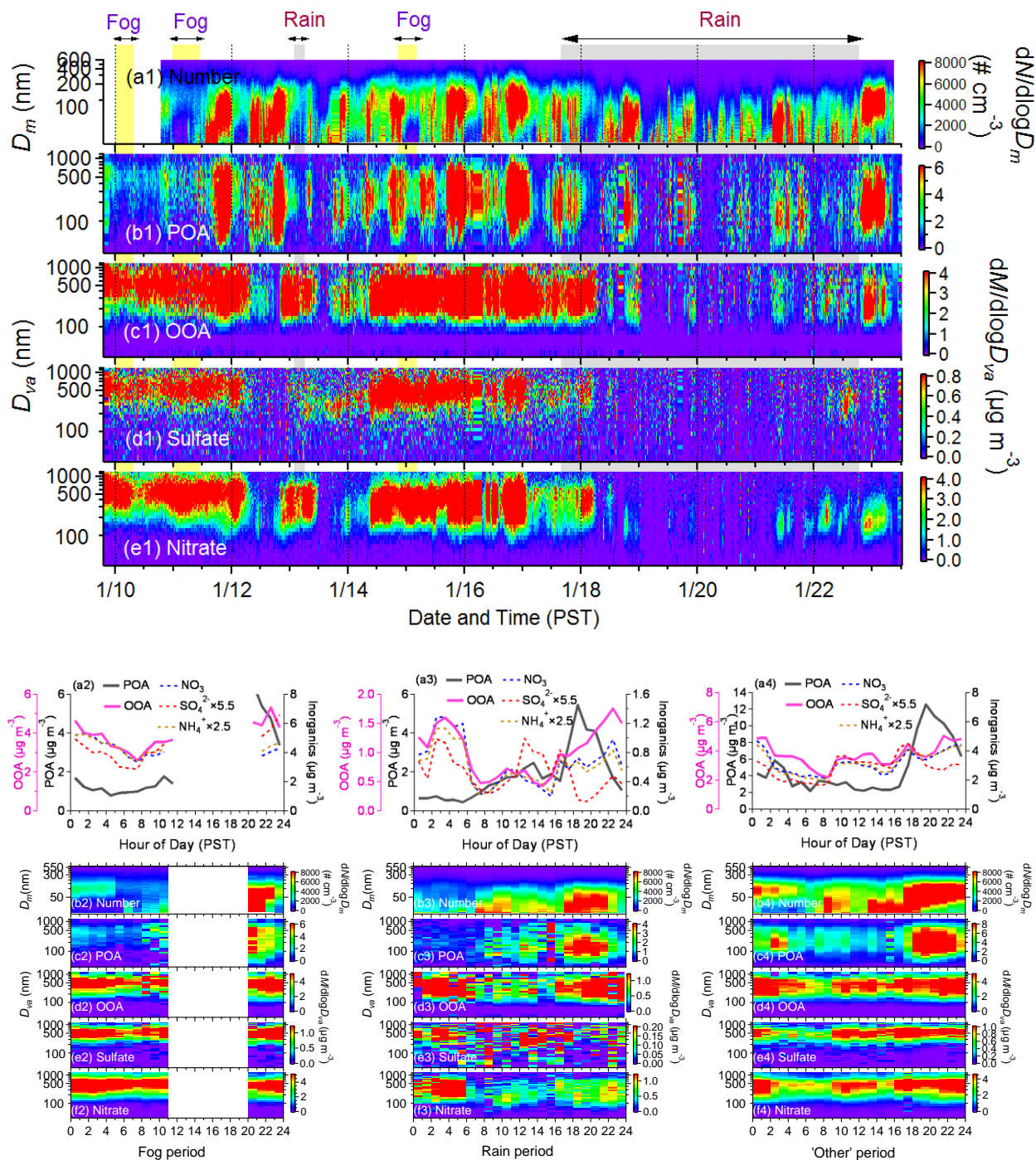


Fig. S2. Temporal variations of the number distributions measured by the SMPS (a1), and mass-based size-distributions of POA, OOA, sulfate and nitrate measured by the AMS (b1–e1), diurnal profiles of sulfate, nitrate, ammonium, POA, OOA (concentrations of sulfate and ammonium are enlarged by factors of 5.5 and 2.5 for clarity), particle number distributions recorded by the SMPS, and mass-based size distributions of POA, OOA, sulfate and nitrate, for the fog (a2–f2), rain (a3–f3) and ‘other’ periods (a4–f4). The classification of different periods is the same as described in Fig.3 of the main text.

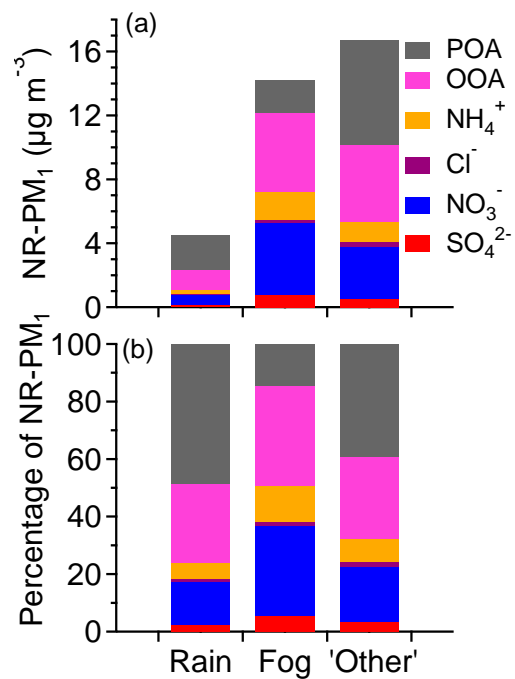


Fig. S3. (a) Average mass concentrations and (b) fractional contributions of aerosol species to the total NR-PM₁ mass during fog, 'other' and rain periods as marked in Fig. 3 of the main text.

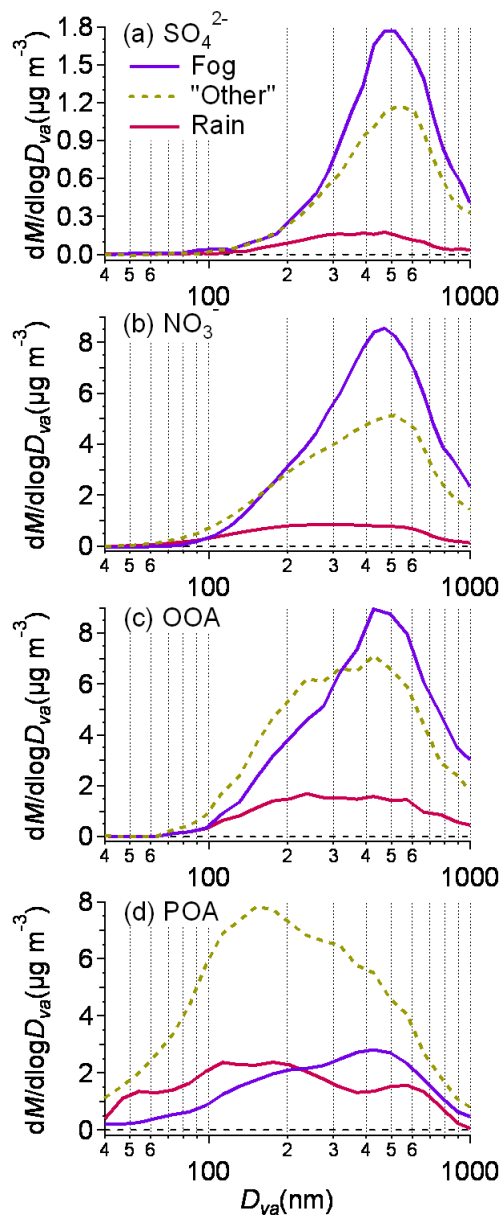


Fig. S4. Averaged mass-based size distributions of (a) sulfate, (b) nitrate, (c) OOA and (d) POA during fog, 'other', and rain periods as marked in Fig. 3 of the main text.

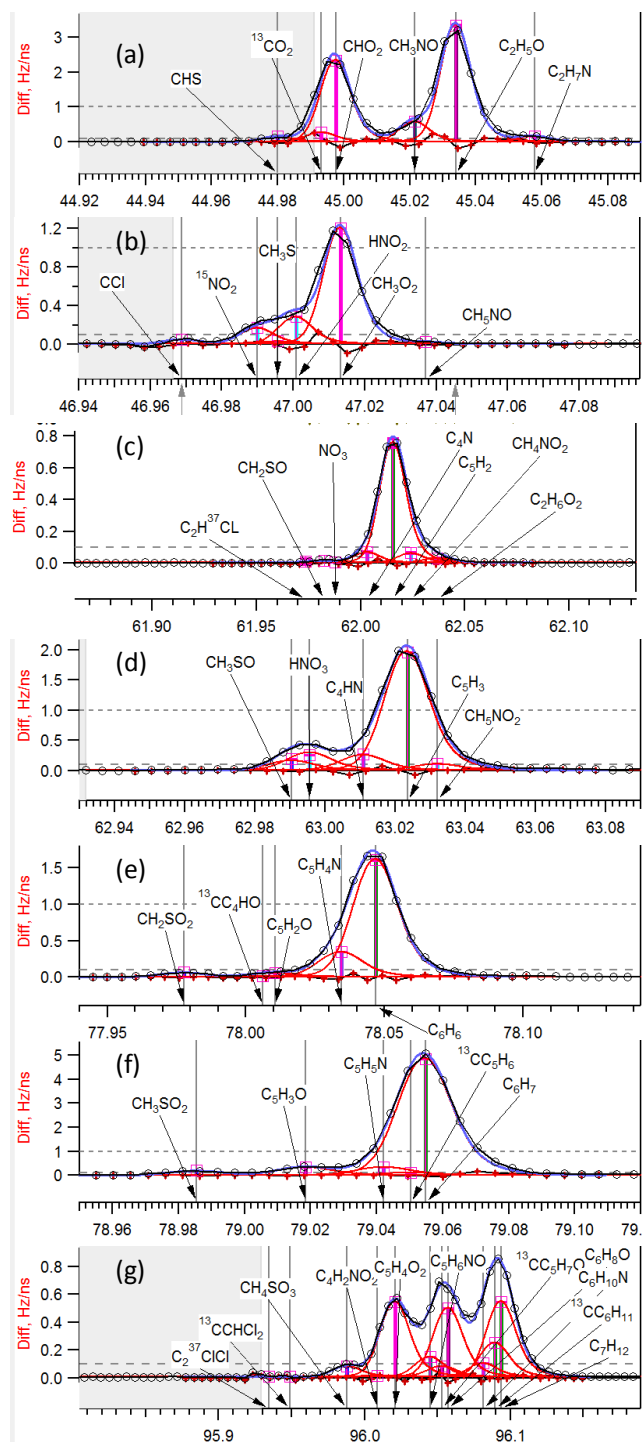


Fig. S5. Raw signals and PIKA fitted peaks of average W-mode mass spectra of the Fresno study of sulfur-containing organic ions (a) CHS^+ (m/z 45), (b) CH_3S^+ (m/z 47), (c) CH_2SO^+ (m/z 62), (d) CH_3SO^+ (m/z 63), (e) CH_2SO_2^+ (m/z 78), (f) CH_3SO_2^+ (m/z 79) and (g) CH_4SO_3^+ (m/z 96) in the AMS raw and fitted mass spectra.

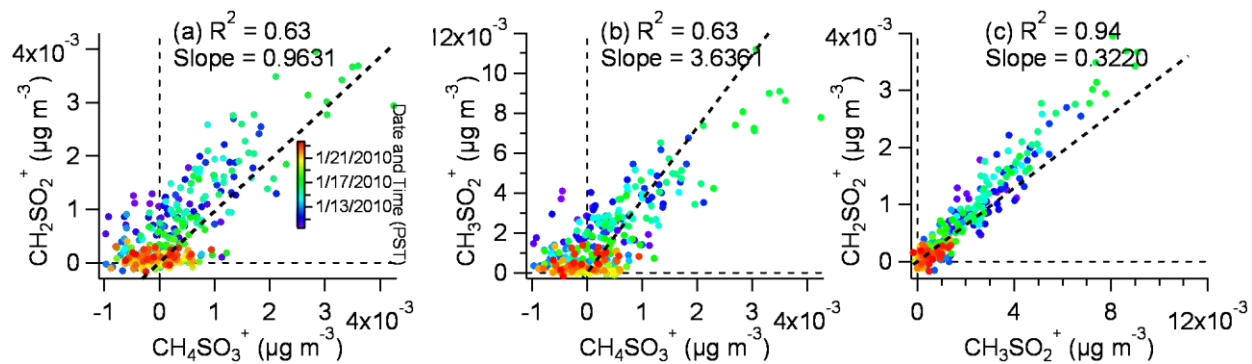


Fig. S6. Scatter plots of (a) CH_2SO_2^+ v. CH_4SO_3^+ , (b) CH_3SO_2^+ v. CH_4SO_3^+ , and (c) CH_2SO_2^+ v. CH_3SO_2^+ . Note the mass concentrations of the ions are averaged on an hourly basis to improve signal-to-noise ratios, especially for CH_4SO_3^+ .

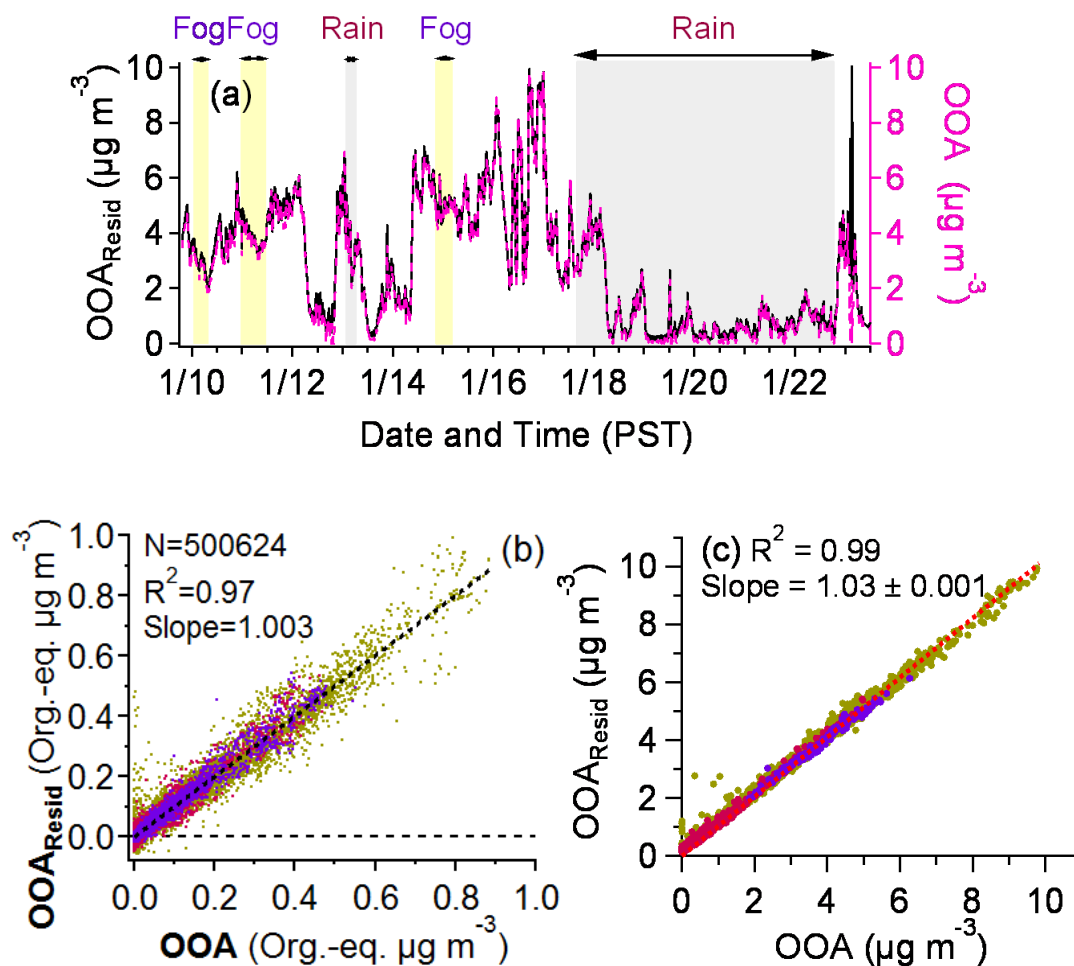


Fig. S7. (a) Time series of the $\text{OOA}_{\text{resid}}$ after subtracting POA contributions from the bulk OA (details are presented in the main text), and the OOA resolved from PMF (the study period are differentiated) (b) scatter plot of all elements in $\text{OOA}_{\text{resid}}$ v. PMF resolved OOA and (c) scatter plot of time series of $\text{OOA}_{\text{resid}}$ v. PMF resolved OOA. The study period is differentiated into three periods as in Fig. 3 of the main text in (a), and the data points are classified into the three different periods in (b) and (c).

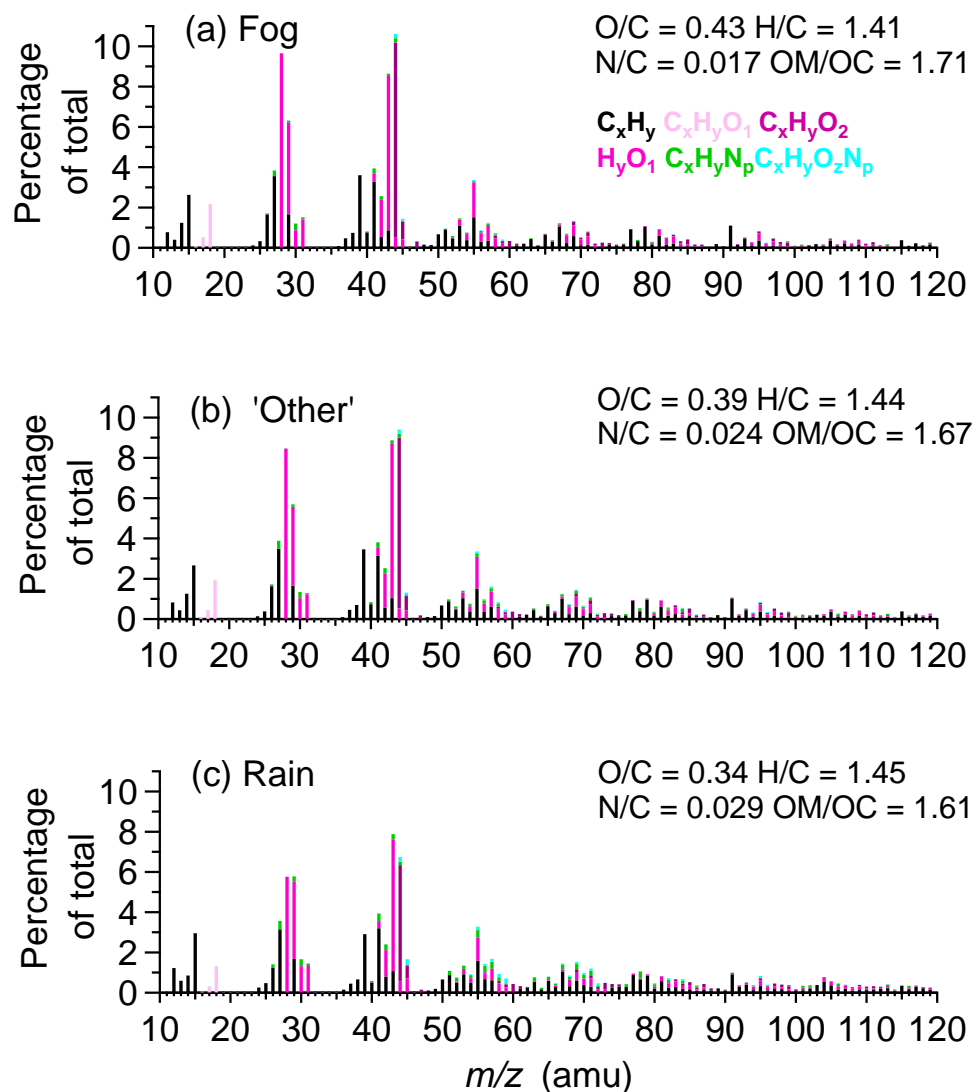


Fig. S8. (a–c) Average high resolution mass spectra of the OOA_{resid} during fog, ‘other’ and rain periods as marked in Fig.3 of the main text.